Comparison of Methanethiol Adsorption on Ag(110) and Cu(110)—Chemical Issues Related to Self-Assembled Monolayers

Jae-Gook Lee, Junseok Lee, and John T. Yates, Jr.*

Surface Science Center, Department of Chemistry, University of Pittsburgh, Pittsburgh, Pennsylvania 15260

Received: June 25, 2003; In Final Form: October 28, 2003

The adsorption and thermal decomposition of methanethiol (CH_3SH) on Ag(110) and on Cu(110) surfaces have been investigated by low energy electron diffraction, Auger electron spectroscopy, and temperature programmed desorption methods. On the clean Ag(110) surface, methanethiol nondissociatively adsorbs at 25 K, forming a (2×1) overlayer structure and then molecularly desorbs at ~140 K. On the partially sulfur-covered Ag(110) surface, methanethiol readily decomposes below 240 K, producing CH_4 (g), H_2S (g), and sulfur atoms on the surface as well as small amounts of carbon. The sulfur overlayer formed by the decomposition of methanethiol exists as a p(3×2) ordered structure at the saturation coverage of sulfur. On this fully sulfur-covered Ag(110) surface, the thermal decomposition of methanethiol is completely suppressed. An autocatalytic mechanism involving silver sites activated by neighboring adsorbed sulfur is proposed to explain the sulfur-catalyzed thermal decomposition reaction of methanethiol on Ag(110). In contrast, on the clean Cu(110) surface, methanethiol decomposes below 320 K, producing CH_4 (g) and C_2H_6 (g), and leaving sulfur overlayers, either a c(2×2) structure at low coverage or a c(8×2) structure at high coverage. A complete layer of chemisorbed sulfur suppresses further methanethiol decomposition on both the silver and the copper surfaces.

1. Introduction

The chemisorption of alkanethiol compounds on metal surfaces has been an interesting topic in the past two decades because alkanethiol self-assembled monolayers (SAMs) offer potential applications in many fields, such as corrosion inhibition, wear protection, wetting, lubrication, chemical sensors, molecular electronics, etc.[1−6] In general, the SAM consists of three parts: a headgroup that strongly binds to the substrate, a surface group that constitutes the outer surface of the molecular layer, and a chain group that connects headgroup and surface groups. The balance between the headgroup−substrate and the intermolecular interactions of chain groups ultimately determines the molecular structure and physical properties of alkanethiol SAMs. The headgroup-substrate interaction plays a predominant role in this balance and the structure of the self-assembled system, which is mainly determined by the choice of the substrate.[1−3,7,8]

There are many studies which address the molecular orientation and ordering of long and short chain alkanethiolate monolayers on various substrates, such as copper, silver, and gold.[8−12] Among these surfaces, the adsorption of alkanethiols on gold and silver surfaces has been extensively investigated by various techniques, including FTIR,[9] Raman spectroscopy,[13] LEED,[14] XPS,[8,15−18] GIXD,[19] X-ray and He diffraction,[10] and STM.[14] In general, it is believed that alkanethiol adsorption on surfaces, such as gold and silver, takes place through S−H bond cleavage to provide the thiolate moiety that attaches to the metal surface through the S atom as an anchor.[14,20,21]

On many transition metals, such as Ni,[22,23] Cu,[24,25] W,[26,27] and Mo,[28,29] alkanethiol S−H bond cleavage occurs generally at relatively low temperature around 100 K, producing the chemisorbed thiolate species, and C−S bond cleavage occurs at higher temperature without producing sulfur-containing gaseous species. However, on relatively inactive metals, such as gold, S−H bond scission is reported to occur incompletely and C−S bond cleavage usually occurs at a temperature around ~400 K, which is higher than that of the more reactive metals.[20,21,30]

It is known that alkanethiols on silver are slightly more reactive than on gold.[14,20,21] Therefore, on silver, the S−H bond of an alkanethiol is expected to dissociate to form alkanethiolate on the surface. As an example, the reactivity of ethanethiol on Ag(110) has been reported by Jaffey et al.[21] In their paper, they report that the S−H bond of ethanethiol dissociates within the temperature range of 100 to 300 K to form thiolate, which was thermally stable to 400 K. At higher temperatures, ethanethiolate decomposes to form mainly ethylene and ethane, and sulfur remains on the surface.

Here, we report the comparative study of the adsorption and thermal decomposition of methanethiol, which is the simplest alkanethiol, on the Ag(110) and Cu(110) surfaces using surface science techniques: temperature programmed desorption (TPD), low energy electron diffraction (LEED), and Auger electron spectroscopy (AES). In contrast to current assumptions, the surprising result is that CH_3SH does not dissociate upon chemisorption on clean Ag(110). The undissociated molecule desorbs at ~140 K. Only when a partially sulfur-covered Ag(110) surface is exposed to CH_3SH does thermal decomposition occur below 240 K, producing CH_4, H_2S, adsorbed S atoms, and a trace of adsorbed carbon. This process is demonstrated to be autocatalytic. These results are in contrast to CH_3SH behavior on clean Cu(110), where CH_3SH dissociation occurs below 320 K leaving sulfur atoms.

These results are of importance in understanding the self-assembly of alkanethiol layers on silver where it has been

* To whom correspondence should be addressed.

10.1021/jp030787q CCC: $27.50
Published on Web 01/07/2004

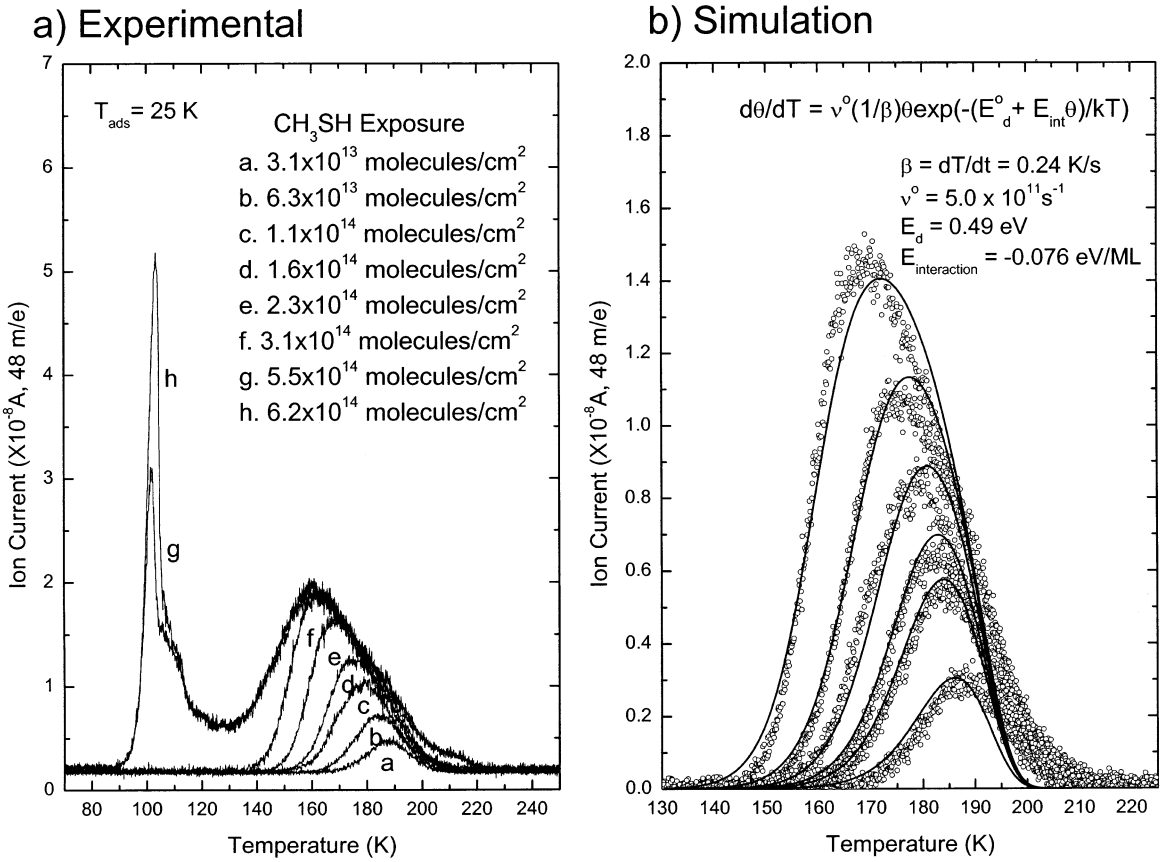

Figure 1. Thermal desorption spectra (taken at m/e = 48 amu/e) of methanethiol on the clean Ag(110) surface. Heating rate = 0.224 K/s. Exposures: (a) 3.1×10^{13} molecules/cm^2; (b) 6.3×10^{13} molecules/cm^2; (c) 1.1×10^{14} molecules/cm^2; (d) 1.6×10^{14} molecules/cm^2; (e) 2.3×10^{14} molecules/cm^2; (f) 3.1×10^{14} molecules/cm^2; (g) 5.5×10^{14} molecules/cm^2; and (h) 6.2×10^{14} molecules/cm^2. (b) Simulation results, compared to experimental points for coverages below 1 ML.

commonly assumed that S−H bond scission occurs on the clean surface at room temperature.

2. Experiment

The adsorption and thermal decomposition of methanethiol on Ag(110) and Cu(110) surfaces has been studied in two different ultrahigh vacuum (UHV) chambers. Each chamber is equipped with basically the same measurement capabilities: a pulse counting LEED apparatus, an Auger spectrometer, and a UTI 100 C quadrupole mass spectrometer (QMS).

The experiments on Ag(110) were performed in a UHV chamber with a base pressure below 6×10^{-11} Torr. The Ag single crystal, a cylindrical disk 3 mm thick, with a diameter of 10 mm, was oriented to within ±0.5° of the ⟨110⟩ plane. The crystal could be cooled to 25 K using a closed-cycle helium cryogenic system and heated to 800 K by resistive heating.

The experiments on the Cu(110) crystal were performed in another ultrahigh vacuum chamber with a base pressure below 2×10^{-10} Torr. The Cu crystal, a cylindrical disk 3 mm thick, with a diameter of 10 mm, was oriented to within ±0.22° of the ⟨110⟩ plane. The Cu crystal could be cooled to 80 K using liquid nitrogen and heated to 900 K by resistive heating.

The silver crystal was exposed to methanethiol (99%, Aldrich) at 25 K for LEED AES and TPD measurements. Exposure was carried out using a calibrated microcapillary array beam doser which produces uniform surface layers while maintaining low background pressure during adsorption.[31] The adsorption flux from this doser to the crystal for methanethiol was in the range 3.0×10^{12}−1.2×10^{13} molecules/cm^2 s, using a calculated interception factor of 0.06, based on the geometry of the doser and the crystal.[31]

The copper crystal was exposed to the methanethiol at 80 K also using a capillary array beam doser. Typically, the adsorbate flux employed was in the range 2.0×10^{12}−1.0×10^{13} molecules/cm^2 s.

The clean crystal samples were prepared by cycles of argon-ion bombardment followed by annealing, and the cleanliness was examined by AES. The Auger spectrum shows no detectable impurities and especially no signs of sulfur near 152 eV after the cleaning procedure. The level of sulfur detection is for Ag (0.23 atom percent) and for Cu (0.15 atom percent) in the depth of Auger detection.

3. Results

3.1. Adsorption of Methanethiol on the Clean Ag (110)−TPD and LEED Results. Figure 1a shows a series of TPD spectra of adsorbed methanethiol on the clean Ag(110) surface at 25 K. After several thermal desorption experiments involving methanethiol were performed, sulfur accumulation on the surface was detected by AES. To remove sulfur contamination from the surface after desorption, the Ag(110) crystal was cleaned by argon-ion bombardment and annealed to 773 K between each TPD measurement. At a methanethiol exposure of 3.1×10^{13} molecules/cm^2, the methanethiol molecular desorption process was observed with a peak maximum at a temperature of 187 K. As the exposure of methanethiol increases, the peak maximum continuously shifts toward lower temperature. At a methanethiol exposure of 5.5×10^{14} molecules/cm^2, an additional sharp desorption peak appears at 103 K, which

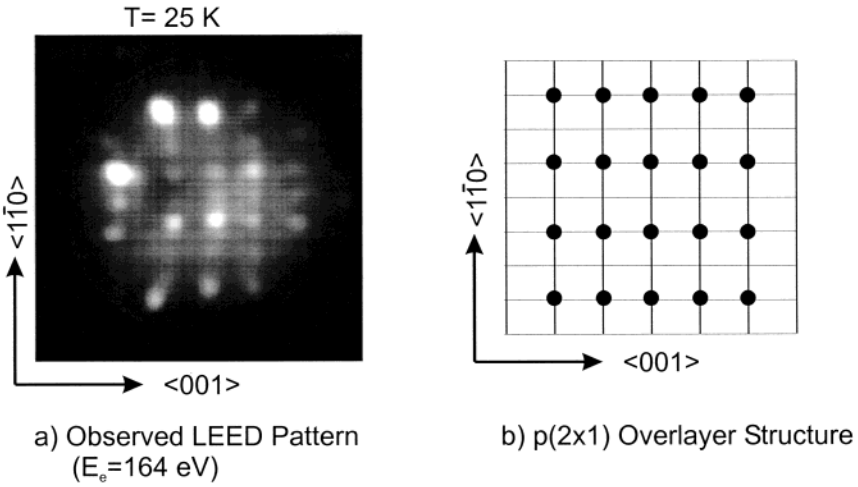

Figure 2. LEED pattern from adsorbed methanethiol on the clean Ag(110) surface at the saturation coverage. Adsorption $T = 25$ K; Heated to 100 K.

originates from the second-layer of methanethiol. On the clean Ag(110) surface, the methanethiol molecule adsorbs and desorbs molecularly without producing any other gaseous products.[32]

TPD spectra in the range of exposures between 3.1×10^{13} molecules/cm^2 and 2.3×10^{14} molecules/cm^2 were assumed to fit first-order desorption kinetics. The spectra were simulated by a numerical method on the basis of the Polanyi−Wigner equation:

$$R_{\mathrm{des}} = (\nu^0/\beta)\theta \exp[-(E_{\mathrm{d}}^0 + E_{\mathrm{int}}\theta)/kT] \qquad (1)$$

where R_{des} is the desorption rate, expressed as $-\mathrm{d}\theta/\mathrm{d}T$, θ is the fractional coverage, ν^0 is the frequency factor, $\beta = \mathrm{d}T/\mathrm{d}t$, E_{d}^0 is the zero-coverage desorption activation energy, and E_{int} is the mutual interaction energy of the adsorbates. The simulation results are shown in Figure 1b in the below-monolayer coverage regime. From the optimal fits, $\nu^0 = 5.0 \times 10^{11}$ s^{-1}, $E_{\mathrm{d}}^0 = 0.49$ eV, and $E_{\mathrm{int}} = -0.076$ eV/monolayer were obtained. The interaction energy is repulsive.

A p(2 × 1) LEED pattern from the methanethiol overlayer was observed at an electron beam energy of 164 eV, as shown in Figure 2. The LEED pattern was obtained after a methanethiol exposure of 3.5×10^{14} molecules/cm^2 on the clean Ag(110) surface at 25 K followed by heating of the surface to 100 K. This p(2 × 1) LEED pattern disappeared at the desorption temperature of methanethiol ($T = \sim$140 K), which indicates that the p(2 × 1) LEED pattern originates from the adsorbed methanethiol overlayer structure.

3.2. Sulfur Accumulation on the Sulfur-Covered Ag(110) Surface—AES, TPD, and LEED Results. The observation of small amounts of sulfur accumulation on the surface after measuring several TPD spectra indicates that thermal decomposition of methanethiol occurs inefficiently on the surface. To investigate quantitatively the amount of sulfur remaining on the surface after thermal desorption experiments, a series of AES measurements was performed after a repeated series of constant exposures (3.0×10^{14} CH_3SH molecules/cm^2) at 25 K, which were followed by thermal treatment up to 773 K, without intermediate surface cleaning. The insert in Figure 3 shows the development of the Auger spectra of sulfur during the repeated measurements. For the first cycle of the experiment, the intensity of the sulfur Auger peak at 152 eV does not increase, compared to that of the observed on the clean Ag(110) surface. As the number of exposure and heating cycles increases, the intensity of the sulfur Auger peak increases gradually up to the ninth or tenth cycle of exposure. Figure 3 shows the sulfur accumulation (measured by the peak-to-peak AES intensity of sulfur) during the repeated exposure of the Ag(110) surface to methanethiol and heating. A sigmoid-shaped curve is observed. The rate of sulfur deposition reaches its maximum between the fifth and the sixth cycle and decreases as the saturation point is approached. In the Auger spectrum, a small amount of carbon was also detected by the subtraction of the clean surface Auger spectrum. We could not measure quantitatively the intensity of carbon due to overlap by the silver Auger signal. However, the intensity of the carbon Auger peak did not increase strongly during repeated methanethiol adsorption and desorption experiments.

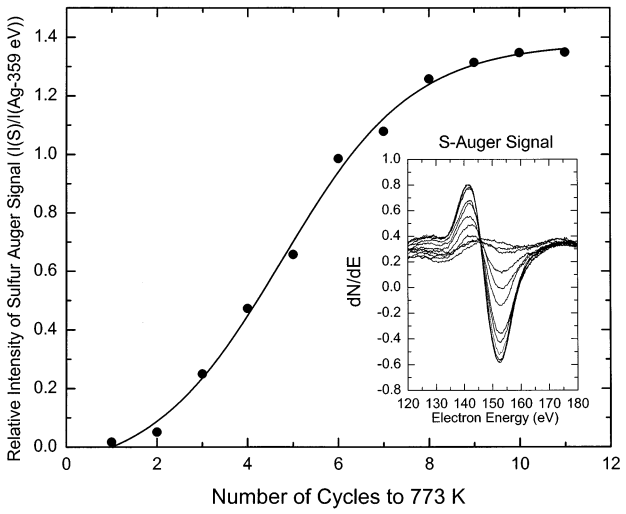

Figure 3. Accumulation of sulfur produced by thermal decomposition of methanethiol on Ag(110) in cyclic experiments involving adsorption-heating, adsorption-heating···. Each cycle involves a CH_3SH exposure of 3.0×10^{14} molecules/cm^2 followed by heating to 773 K. The line is drawn to guide the eye. For kinetic fits see Figure 9.

A series of TPD experiments was also carried out to monitor the evolution of the gaseous products as a result of thermal decomposition of methanethiol during sulfur accumulation on the surface. In contrast to the results on the ***clean*** Ag(110) surface, the evolution of methane (CH_4) at ∼400 K and hydrogen sulfide (H_2S) in the temperature range of 140−220 K was observed on the partially sulfur-covered Ag(110) surface. Figure 4 presents the total gas evolution for CH_3SH, CH_4, and H_2S as repeated cycles of adsorption and heating to 773 K occur.

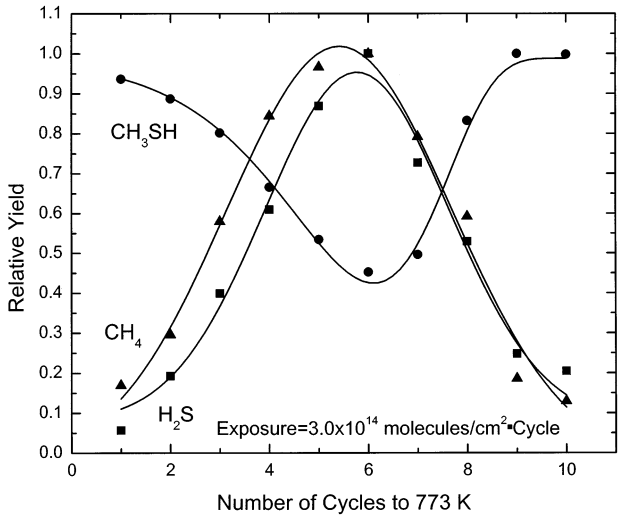

Figure 4. Relative yields in the evolution of gaseous species from thermal decomposition of methanethiol on Ag(110). The lines are drawn to guide the eye.

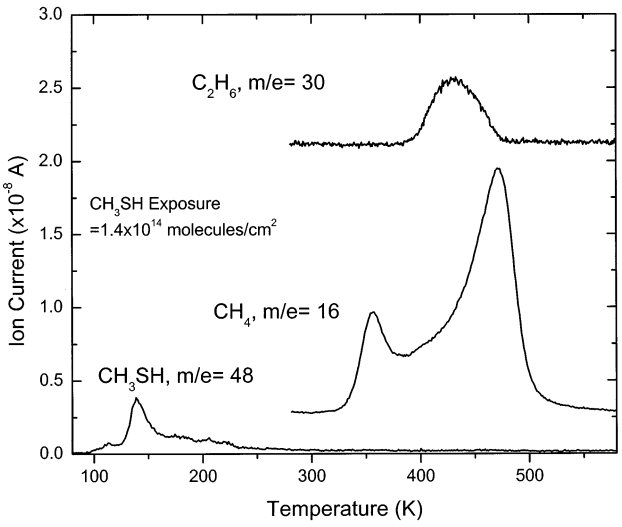

Figure 5. TPD spectra of methanethiol on clean Cu(110) at exposures of 1.4×10^{14} molecules/cm^2. Adsorption temperature = 80 K

It is found that the evolution of CH_4 and H_2S reaches a maximum point when the sulfur accumulation occurs at a maximum rate and that the CH_3SH desorption yield behaves in an opposite manner to the CH_4 and H_2S yields. On the sulfur-saturated surface, no CH_4 or H_2S evolution was observed.

No particular LEED pattern was observed from the adsorbed methanethiol and adsorbed sulfur on the partially sulfur-covered Ag(110) surface. For the sulfur-saturated surface, the adsorbed sulfur atoms show a p(3 × 2) long range ordered structure, which is consistent with other studies.[33]

3.3. Thermal Decomposition of Methanethiol on the Cu-(110) Surface. In contrast to observations on the clean Ag-(110), adsorbed methanethiol on the clean Cu(110) mostly decomposes to methane and ethane, leaving sulfur on the surface. Figure 5 shows a TPD spectrum of methanethiol adsorbed at 80 K at an exposure of 1.4×10^{14} molecules/cm^2 on the clean Cu(110) surface. A ***small*** desorption peak for methanethiol was observed at 140 K. Methane, one of the decomposition products, desorbed with two desorption features at 360 and 470 K and an ethane desorption peak appeared at 430 K. No desorption of H_2 and H_2S was detected during the TPD measurements.

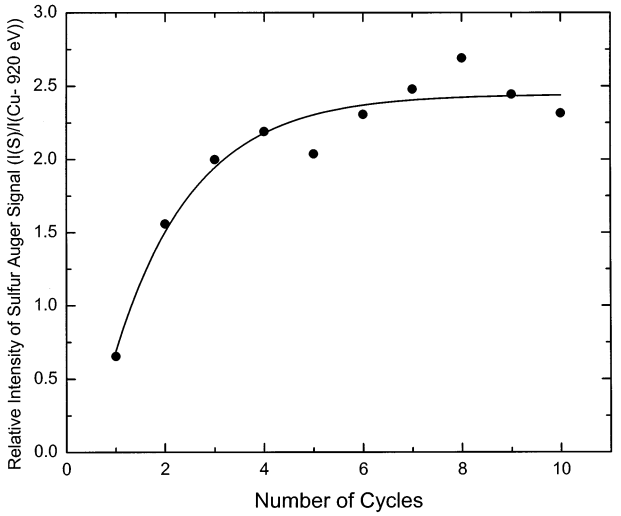

Figure 6. Accumulation of sulfur produced by thermal decomposition of methanethiol on Cu(110). The line is drawn to guide the eye.

LEED experiments were performed to investigate the ordered structures of adsorbed methanethiol and of adsorbed sulfur on Cu(110). No particular LEED pattern was observed for adsorbed methanethiol at various exposures on the clean Cu(110) surface. The LEED study for adsorbed methanethiol on the S-covered surface could not be carried out in detail due to the interference of the underlying sulfur overlayer structure.

Two LEED patterns for the sulfur overlayer during the sulfur accumulation were observed. A c(2 × 2) LEED pattern was obtained at a relative low coverage of sulfur on Cu(110) at 80 K. At higher coverage, the c(2 × 2) LEED pattern converted to a c(8 × 2) pattern.

To investigate the profile of sulfur atom accumulation by decomposition of methanethiol, repeated doses of methanethiol molecules (1.4×10^{14} molecules/cm^2) were employed without cleaning the surface after each AES measurement, in the same way as in the experiment performed on Ag(110). After the first adsorption and desorption of methanethiol on the clean Cu(110) surface, a substantial amount of sulfur accumulation was detected as shown in Figure 6. The accumulation of sulfur occurs most efficiently at the first cycle of adsorption and desorption of methanethiol. The amount of sulfur on the copper surface increases sharply as the cycles of exposing and annealing are repeated. After the fifth or sixth cycle of exposing and heating, the intensity of the sulfur Auger peak was unchanged for successive experiments. In the Auger spectrum, although a small amount of carbon also was detected, the carbon intensity did not increase during repeated methanethiol adsorption and desorption experiments.

The profile for the major desorption products generated by methanethiol decomposition on the Cu(110) surface is quite different from that of methanethiol on Ag(110) during the repeated exposure experiments. For Cu(110) the yield of methane and ethane dramatically decreases as sulfur accumulation occurs without showing any maximum as shown in Figure 7. For Cu(110), the activity for CH_3SH decomposition steadily ***decreases*** as S accumulates; in contrast, for Ag(110), the activity for CH_3SH decomposition ***increases*** initially as S accumulates.

4. Discussion

4.1. Nondissociative Adsorption of Methanethiol on Clean Ag(110). The adsorption and desorption of methanethiol have been thoroughly studied on the clean Ag(110) surface. The methanethiol molecule at or below monolayer coverage desorbs

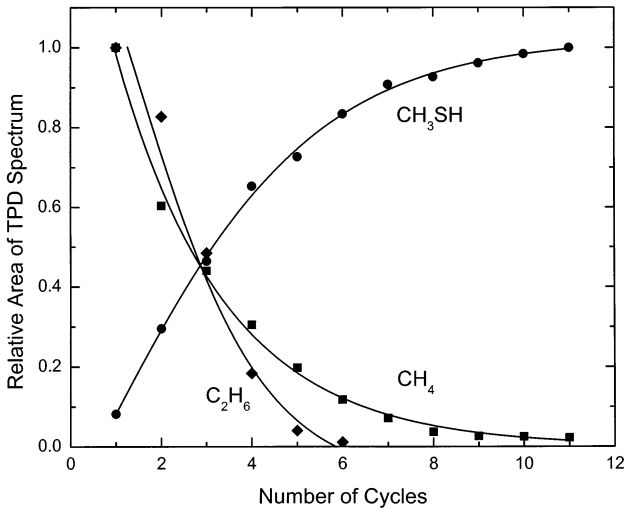

Figure 7. The evolution of gaseous species from thermal decomposition of methanethiol on Cu(110). Each cycle involves a CH_3SH exposure of 1.4×10^{14} molecules/cm^2 followed by heating to 673 K. The lines are drawn to guide the eye.

at ~140 K without leaving detectable sulfur on the surface. Methanethiol desorbs by first-order desorption kinetics, indicating that recombinative desorption does not take place. A relatively small desorption activation energy (0.49 eV) is observed for adsorbed methanethiol on Ag(110). The shift of the desorption maximum in TPD toward lower temperature indicates that the repulsive adsorbate−adsorbate interaction is a dominant feature until the ordered p(2 × 1) overlayer structure forms, and a repulsive interaction energy of 0.076 eV/ML has been measured. This contrasts with the adsorptive behavior of long chain alkanethiols, where attractive intermolecular energies are observed.[34]

4.2. Sulfur-Induced Decomposition of Methanethiol on the Sulfur-Covered Ag(110) Surface. The following important features were observed for methanethiol adsorption and desorption on Ag(110): (1) methanethiol does not decompose on the clean Ag(110) surface; (2) methanethiol readily decomposes on the partially sulfur-covered Ag(110) surface and produces the gaseous products, CH_4 and H_2S; (3) a very small portion of adsorbed methanethiol decomposes at the initial stage (the first and second cycle) of the repeated exposure experiment (this probably happens on defect sites on the Ag(110) crystal); (4) on the sulfur-saturated Ag(110) surface, the decomposition reaction is completely deactivated.

Based on the above observations, although the structural aspects are speculative, we propose an adsorption and decomposition model for the methanethiol on the silver surface as schematically shown in Figure 8. Presumably, the chemisorbed methanethiol interacts with the surface silver atom through one or two sulfur lone-pair orbitals. It is clear from simple thermodynamic arguments that the silver surface should be able to dissociate the S−H bond of methanethiol. However, from our experimental observations, methanethiol adsorbs nondissociatively on the clean Ag(110) probably as a result of a high activation energy barrier to S−H bond scission. The relatively small measured desorption energy of methanethiol (0.49 eV) on silver indicates that methanethiol interaction with silver is not strong enough to induce S−H bond cleavage.

We attribute the initial CH_3SH dissociation process, presumably producing CH_3S(a) and H(a), to the presence of random defect sites on the Ag(110) surface. These sites may bond to CH_3SH more strongly than Ag(110) sites, allowing the molecule to remain on the surface to higher temperatures, where activated S−H bond cleavage can occur. The adsorbed S atom then acts autocatalytically to decompose neighboring CH_3SH molecules which have been adsorbed in our cyclic experiments. Possibly the stable SH(a) (sulfhydryl) species (H−S bond energy = 3.69 eV[35]) is produced by abstracting an H atom from neighboring H−S−CH_3 species. This process is thermodynamically preferred to the formation of the Ag−H bond (bond energy = 2.15 eV[36]).

On the fully sulfur-covered Ag(110) surface, CH_3SH dissociation does not occur, although CH_3SH adsorption does occur.

We invoke the formation of surface−SH species in the decomposition mechanism. The disproportionation reaction SH(a) + SH(a) → H_2S(g) + S(a) is postulated to be responsible for H_2S evolution and contributes to the lack of formation of adsorbed H(a) on the surface and hence the lack of H_2(g) desorption.

It is interesting to compare the dissociation ability of CH_3SH with C_2H_5SH on Ag(110). Jaffey et al.[21] report partial C_2H_5SH dissociation in the temperature range of 100−300 K where on clean Ag(110) we observe little or no CH_3SH dissociation. Two rationales to explain this difference may be suggested:

(1) The experiments with C_2H_5SH on Ag(110) were influenced by tiny coverages of sulfur which induced the autocatalytic decomposition reaction.

(2) The lability of the S−H bond is influenced by the character of the alkyl group. The C_2H_5 group induces greater S−H bond reactivity than the CH_3 group (for similar reasons, the pK_a of ethanethiol (10.61) is smaller than that of methanethiol (pK_a = 10.70).[37]

4.3. Autocatalytic Mechanism of CH_3SH Dissociation−Ag(110). Based on the above adsorption model for methanethiol on Ag(110), a kinetic expression has been derived using the following assumptions for methanethiol decomposition on the Ag(110) surface to explain the behavior of the sulfur accumulation on the Ag surface in the repeated exposure experiment:

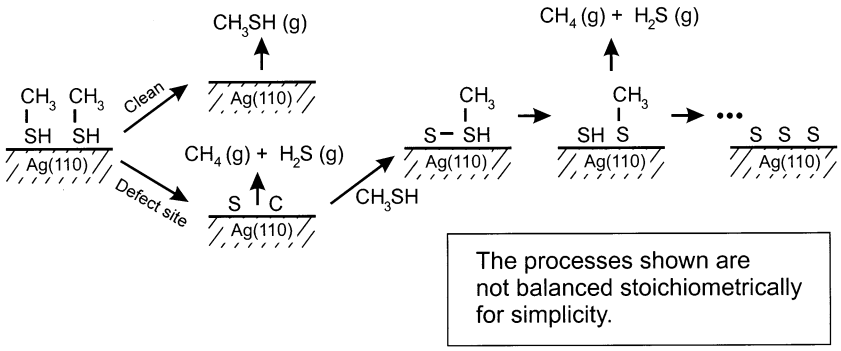

Figure 8. Schematic for methanethiol decomposition on Ag(110).

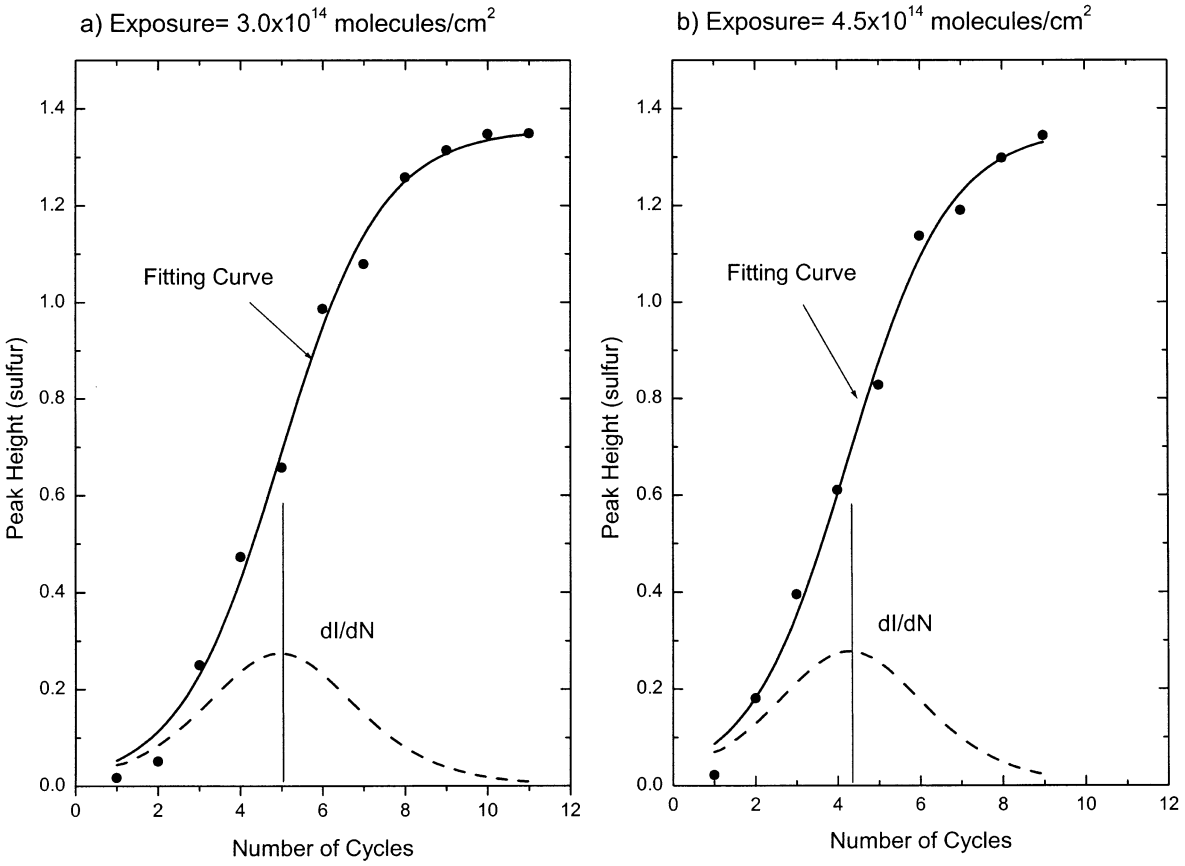

Figure 9. Simulation of sulfur accumulation on the Ag(110) surface using the autocatalytic CH_3SH decomposition mechanism by adsorbed sulfur. (a) Each exposure = 3.0×10^{14} molecules/cm^2. (b) Each exposure = 4.5×10^{14} molecules/cm^2. I = magnitude of fitting curve.

(1) the adsorbed methanethiol molecule is localized and does not migrate on the surface before desorption occurs; therefore, the number of molecules adsorbed at neighbor sites to individual sulfur atoms is fixed; (2) the reaction occurs only at the boundary between the isolated chemisorbed sulfur atom and the clean silver surface (autocatalytic reaction by sulfur); (3) the methanethiol molecule does not decompose on the surface completely covered by sulfur; (4) the amount of reactant that actually reacts in each cycle of repeated exposure is small. The rate expression is

$$-\frac{d\theta_m}{dN} = C\theta_m\theta_s \qquad (2)$$

where θ_m is the coverage of methanethiol molecules on the clean surface, θ_s is sulfur coverage on the surface, N is the number of repeated exposures, and C is a parameter which is related to the reaction rate constant. As the decomposition reaction occurs, the clean surface area will be replaced by the sites covered with sulfur. Therefore, the relation $\theta_m^0 - \theta_m = \theta_s - \theta_s^0$ will be satisfied where θ_s^0 is the coverage of S after a given cycle. Using this relation, the following expression was obtained for the accumulation of sulfur:

$$\theta_s = \frac{\theta_m^0 + \theta_s^0}{1 + \frac{\theta_m^0}{\theta_s^0}\exp[-C(\theta_m^0 + \theta_s^0)N]} \qquad (3)$$

where θ_s^0 is the initial sulfur coverage and θ_m^0 is the initial coverage of the clean surface occupied by methanethiol molecules, in any cycle.

The sulfur Auger signal is proportional to the sulfur coverage, θ_s. Therefore, if we consider a proper proportionality constant (k), we can apply eq 3 to the cyclic experiments where chemisorbed sulfur accumulates. We performed the fitting procedure using the above formula to fit the AES data obtained for two different cyclic experiments involving exposures of methanethiol = 3.0×10^{14} molecules/cm^2 cycle (below monolayer coverage) and 4.5×10^{14} molecule/cm^2 cycle (above monolayer coverage), as shown in Figure 9. For the optimal fitting results, we obtain very similar values for $\theta_m^0 + \theta_s^0 = 1.45k$, and $C = 0.6k$ in both cases. The value for $\theta_m^0/\theta_s^0 = 55$ and 33, respectively.

The derived eq 3 describes well the behavior of the sulfur accumulation for each of the cyclic experiments. Interestingly, we obtained the same reaction parameter C, for both cyclic experiments. This indicates that the sulfur accumulation reaction does not depend on the methanethiol exposure ***but depends on the initial sulfur coverage***. In other words, if the methanethiol covers the reaction sites neighboring an adsorbed S atom, the rate of accumulation of sulfur is not affected by additional methanethiol exposure.

Comparing the sulfur accumulation curves for the two cyclic experiments, we see that the rate of S accumulation is accelerated for the experiment involving higher values of θ_s^0, as would be expected.

4.4. Comparison of the Methanethiol Adsorption on Ag(110) to Adsorption on Cu(110)—A Summary. Compared to methanethiol adsorption on Cu(110), there are interesting differences on Ag(110). The most striking difference is that the adsorbed methanethiol does not thermally decompose on the clean Ag(110) surface. On Ag(110), the main products of methanethiol decomposition are methane and hydrogen sulfide,

postulated to initially originate from defect sites interacting with CH_3SH, whereas methane and ethane are major gaseous products on Cu(110). Thermal decomposition of methanethiol on Ag(110) only occurs on the partially sulfur-covered surface, whereas on Cu(110) decomposition occurs on the clean surface.

The differences between the methanethiol adsorption and decomposition on Ag(110) and Cu(110) surfaces are rationalized by the greater affinity of Cu for sulfur compared to Ag, as indicated by the enthalpies of formation of the sulfides (ΔH_f (Ag_2S) = −0.34 eV, ΔH_f (Cu_2S) = −0.82 eV).[35] In fact, the difference of affinity for sulfur leads to the different thermal decomposition pathways of methanethiol on the two different metal surfaces. It is well established that S−H bond dissociation on Cu occurs at $T < 150$ K, as reported in the experiment of Woodruff et al. for Cu(111).[38,39] Because of the lack of reactivity of silver metal compared to copper, methanethiol adsorbs nondissociatively on silver. However, on silver, in the presence of chemisorbed sulfur, S−H bond scission in methanethiol occurs to produce the sulfhydryl species and chemisorbed methanethiolate at low temperature. The lower affinity of silver metal for sulfur makes it possible for two sulfhydryl species to disproportionate to hydrogen sulfide and surface sulfur at relatively low temperature. The methanethiolate species also decomposes into methane gas and chemisorbed sulfur at high temperature. In contrast, CH_3SH decomposes by S−H bond scission at low temperature on clean Cu(110). The strong affinity of Cu for S leads to no evolution of S-containing species from the surface (CH_3SH, H_2S). Accordingly, for CH_3SH decomposition on Cu(110), S accumulates rapidly. The removal of surface hydrogen as H_2S(g) causes CH_4 evolution from CH_3SH(a) on Ag(110) to be shifted to high temperature where C−H bond scission occurs, providing surface hydrogen used to form CH_4(g).

In summary, we find that the methanethiol molecule does not decompose upon adsorption on clean Ag(110). It is likely that random defect sites are effective in causing a small fractional decomposition initially and that adsorbed S atoms then provide neighboring sites with enhanced ability to decompose the CH_3SH molecule by an autocatalytic mechanism. The presence of adsorbed S therefore governs the decomposition of methanethiol on Ag(110). This indicates that in alkanethiol−SAM preparation, surface cleanliness of silver is essential in controlling the formation of the surface layer and that on partially contaminated silver surfaces one may produce a mixed layer of thiolate and thiol species with different surface chemistries.

5. Summary

The following results have been obtained for the interaction of methanethiol both with the clean and the sulfur-covered Ag(110) surface and with the clean and the sulfur-covered Cu(110) surface.

Methanethiol nondissociatively adsorbs on the clean Ag(110) surface, forming a (2 × 1) overlayer structure and desorbs at ∼140 K.

On the partially sulfur-covered Ag(110) surface, methanethiol readily decomposes below 240 K, producing CH_4(g), H_2S(g), and sulfur atoms on the surface. It is likely that an H−S(a) intermediate species is involved in a disproportionate reaction yielding H_2S(g) and S(a).

The sulfur overlayer formed by the decomposition of methanethiol on Ag(110) shows a p(3 × 2) ordered structure at the saturation coverage of sulfur.

An autocatalytic reaction mechanism by sulfur is proposed for the decomposition of methanethiol on Ag(110). The decomposition reaction on Ag(110) occurs at neighbor sites to chemisorbed sulfur atoms.

In contrast, on the clean Cu(110) surface, methanethiol decomposes, producing CH_4(g) and C_2H_6(g), leaving sulfur overlayers in a c(2 × 2) and a c(8 × 2) structure at low and saturation coverage, respectively.

Chemisorbed sulfur at the saturation coverage suppresses further methanethiol decomposition on both the silver and the copper surfaces.

The greater affinity of Cu for sulfur compared to Ag controls the methanethiol adsorption and decomposition mechanism on the two metals.

Acknowledgment. We acknowledge with thanks the support of this work by the Department of Energy, Office of Basic Energy Sciences.

References and Notes

(1) Ulman, A. *An Introduction to Ultrathin Organic Films: Langmuir−Blodgett to Self- Assembly*; Academic Press: Boston, 1991.
(2) Ulman, A. *Chem. Rev.* **1996**, *96*, 1533.
(3) Ulman, A. *Self-Assembled Monolayers of Thiols*; Thin Films; Academic Press: San Diego, CA, 1998; Vol. 24.
(4) Whitesides, G. M.; Manthias, J. P.; Seto, C. T. *Science* **1991**, *254*, 1312.
(5) Dubois, L. H.; Nuzzo, R. G. *Annu. Rev. Phys. Chem.* **1992**, *43*, 437.
(6) Holmlin, R. E.; Haag, R.; Chabinyc, M. L.; Ismagilov, R. F.; Cohen, A. E.; Terfort, A.; Rampi, M. A.; Whitesides, G. M.; *J. Am. Chem. Soc.* **2001**, *123*, 5075.
(7) Frey, S.; Stadler, V.; Heister, K.; Eck, W.; Zharnikov, M.; Grunze, M.; Zeysing, B.; Terfort, A.*Langmuir* **2001**, *17*, 2408.
(8) Rong, H.-T.; Frey, S.; Yang, Y.-J.; Zharnikov, M.; Buck, M.; Wühn, M.; Wöll, C.; Helmchen, G. *Langmuir* **2001**, *17*, 1582.
(9) Laibinis, P. E.; Whitesides, G. M.; Allara, D. L.; Tao, Y.-T.; Parikh, A. N.; Nuzzo, R. G. *J. Am. Chem. Soc.* **1991**, *113*, 7152.
(10) Fenter, P.; Eisenberger, P.; Li, J.; Bernasek, C. S.; Scoles, G.; Ramanarayanan, T. A.; Liang, K. S.*Langmuir* **1991**, *7*, 2013.
(11) Cavallini, M.; Bracali, M.; Aloisi, G.; Guidelli, R. *Langmuir* **1999**, *15*, 3003.
(12) Riely, H.; Kendall, G. K. *Langmuir* **1999**, ***15***, 8867.
(13) Joo, S. W.; Han, S. W.; Kim, K.*Langmuir* **2000**, *16*, 5391.
(14) Heinz, R.; Rabe, J. P. *Langmuir* **1995**, *11*, 506.
(15) Ishida, T.; Choi, N.; Mizutani, W.; Tokumoto, H.; Kojima, I.; Azehara, H.; Hokari, H.; Akiba, U.; Fujihira, M.*Langmuir* **1999**, *15*, 6799.
(16) Jung, Ch.; Dannenberger, O.; Xu, Y.; Buck, M.; Grunze, M. *Langmuir* **1998**, *14*, 1103.
(17) Heister, K.; Zharnikov, M.; Grunze, M.; Johansson, L. S. O. *J. Phys. Chem. B* **2001**, *105*, 4058.
(18) Castner, D. G.; Hinds, K.; Grainger, D. W. *Langmuir* **1996**, *12*, 5083.
(19) Fenter, P.; Eisenberger, P.; Liang, K. S. *Phys. Rev. Lett.* **1993**, *70*, 2447.
(20) Jaffey, D. M.; Madix, R. J. *J. Am. Chem. Soc.* **1994**, *116*, 3020.
(21) Jaffey, D. M.; Madix, R. J. *Surf. Sci.* **1994**, *311*, 159.
(22) Kane, S. M.; Huntley, D. R.; Gland, J. L. *J. Am. Chem. Soc.* **1996**, *118*, 3781.
(23) Castro, M. E.; White, J. M. *Surf. Sci.* **1991**, *257*, 22.
(24) Sexton, B. A.; Nyberg, G. L. *Surf. Sci.* **1986**, *165*, 251.
(25) Prince, N. P.; Seymour, D. L.; Woodruff, D. P.; Jones, R. G.; Walter, W. *Surf. Sci.* **1989**, *215*, 566.
(26) Benziger, J. B.; Preston, R. E.; *J. Phys. Chem.* **1985**, *89*, 5002.
(27) Mullins, D. R.; Lyman, P. F. *J. Phys. Chem.* **1993**, *97*, 9226.
(28) Roberts, J. T.; Friend, C. M. *J. Chem. Phys.* **1988**, *88*, 7172.
(29) Wiegand, B. C.; Uvdal, P.; Friend, C. M. *Surf. Sci.* **1992**, *279*, 105.
(30) Labinis, P. E.; Fox, M. A.; Folkers, J. P.; Whitesides, G. M. *Langmuir*, **1991**, *7*. 3167.
(31) Yates, J. T., Jr. *Experimental Innovations in Surface Science*; AIP press and Springer-Verlag: New York, 1998; see also Winkler, A.; Yates, J. T., Jr. *J. Vac. Sci. Technol. A* **1988**, ***6***, 2929.
(32) Lee, J.-G.; Lee, J.; Yates, J. T., Jr. *J. Am. Chem. Soc.* (in press).
(33) Rovida, G.; Pratesi, F. *Surf. Sci.* **1981**, *104*, 609.
(34) Nuzzo, R. G.; Dubois, L. H.; Allara, D. L.*J. Am. Chem. Soc.* **1990**, *112*, 558.

(35) Weast, R. C., Ed.; *Handbook of Chemistry and Physics*, 69th ed.; CRC Press: Boca Raton, FL, 1989
(36) Simoes, J. A. M.; Beauchamp, J. L. *Chem. Rev.* **1990**, *90*, 629.
(37) Dean, J. A., Ed.; *Lange's Handbook of Chemistry*, 14th ed.; McGraw-Hill Inc: New York, 1992.
(38) Jackson, G. J.; Woodruff, D. P.; Jones, R. G.; Singh, N. K.; Chan, A. S. Y.; Cowie, B. C. C.; Formoso, V. *Phys. Rev. Lett.* **2000**, *84*, 119.
(39) Toomes, R. L.; Polcik, M.; Kittel, M.; Hoeft, J.-T.; Sayago, D. I.; Pascal, M.; Lamont, C. L. A.; Robinson, J.; Woodruff, D. P. *Surf. Sci.* **2002**, *513*, 437 and references therein.